

Modelling of Diesel Spray Dynamics using LES

C.H. Bong, L.C. Goldsworthy and P.A. Brandner

National Centre for Maritime Engineering & Hydrodynamics
Australian Maritime College, University of Tasmania, Launceston 7250, Australia

Abstract

A non-evaporating high pressure spray of diesel fuel in a pressurised spray chamber is modelled using the CFD code StarCD. Large eddy simulation is used in conjunction with a Lagrangian model for the dispersed phase. Simulations are compared with data on spray penetration, spray width and droplet diameter from an optically accessible instrumented spray chamber. Spray penetration and width as well as droplet diameter are moderately well simulated. It is postulated that the most significant limitation regarding the ability to model real spray behaviour is the restriction on minimum cell size near the nozzle, inherent in the Lagrangian approach.

Introduction

A diesel spray is a complex phenomenon involving multiphase fluid flow, high Reynolds number turbulent flow and large shearing of fluid between the nozzle exit and the surrounding fluid. The large shearing of fluid flow results in the formation of Kelvin-Helmholtz instability. This is thought to be the primary cause of the formation a flow pattern with large eddies that widen the spray. Droplet formation involves rapid atomization due to a combination of cavitation and turbulence inside the injector nozzle and aerodynamically induced breakup [1]. Within a few nozzle diameters downstream of the nozzle exit the liquid forms ligaments which rapidly disintegrate into droplets with aerodynamic forces leading to catastrophic breakup and surface stripping [2,3]. Inter-droplet collisions can result in either coalescence or the generation of smaller droplets [4].

If all these complexities are simulated using fundamental physics, the computation requirement is simply beyond the capability using current generation of computing technology. As a result, various analytical models that work well isolation are combined for simulation of the diesel spray process. Large Eddy Simulation (LES) is a CFD simulation method that resolves the 'greater than grid-size' length scales of fluid flow directly with the Navier-Stokes equations. [5-8] A simple turbulence model is used to resolve smaller lengthscales. This is a good compromise with accuracy that lies between the Reynolds Averaged Navier Stokes (RANS) and Direct Numerical simulation (DNS) methods, the latter method being the most accurate but with high computational cost. In this report, the ability of LES to simulate a diesel spray is studied.

Experimental set up

A constant volume High-Pressure Spray Chamber (HPSC) was used for measurement of long duration, non-evaporating diesel sprays. The chamber and instrumentation are described in [9]. The inside cross-section of the HPSC is a rounded square measuring 120 x 120 mm, with 23 mm fillets. The windows are recessed by 15 mm from the inner surface to reduce contamination with fuel spray. The depth of the chamber is 270 mm with 200 mm x 70 mm window sections. The internal volume is approximately four litres. The injection system utilises a modified Hydraulically Actuated Electronically Controlled Unit Injector (HEUI) with adjustable injection durations from 1 to 20 ms. The injection nozzle used is a single hole type with 240 μ m diameter and 1 mm length. The injection pressure was kept at 109 MPa average throughout all experiments. Chamber gas pressures were 20, 30 and 40 bar. These pressures at room temperature give gas densities similar to a Diesel engine at the

end of the compression stroke. A light sheet from an Nd:YAG laser was used for capturing a cross-section of the spray (Figure 1). A solid state diffuser on the laser was used as the backlight for droplet imaging. A LaVision Imager Intense dual frame CCD camera was used. The sensor has a resolution of 1376 x 1040 pixels and 12 bit intensity depth.

Sample images of the spray were taken using the light-sheet with the camera adjusted to capture the whole spray. A statistically significant number of images were taken at times varying between 0.5 to 10 ms after start of injection at 0.5 ms intervals. These images were used to measure the average cone angle and penetration. To determine spray penetration and cone angle, the spray boundary of each of around 200 backlit images of the whole spray was found by normalising the images, applying a threshold, applying a Canny edge detection algorithm and finally finding the edge closest to the spray centreline.

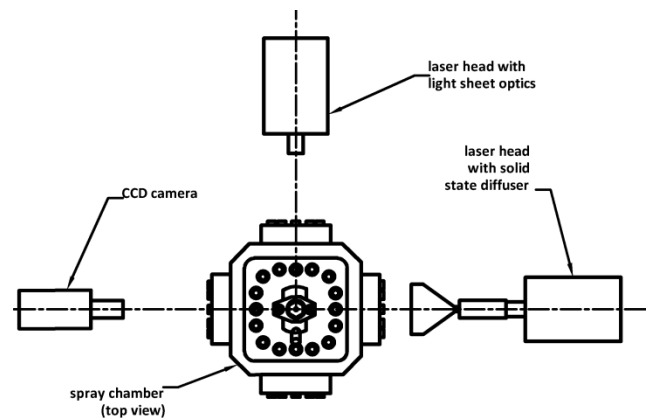


Figure 1 Top down view of the experiment set up.

Dropsizes were measured using a Questar QM-1 long-distance microscope. The minimum working distance of the microscope is 560 mm and it has a focus number equal to 8.7 at that distance. A statistically significant number of droplet images were taken at 5 ms after start of injection at a variety of spray locations (see Figure 2). Other conditions were kept the same as the penetration measurements.

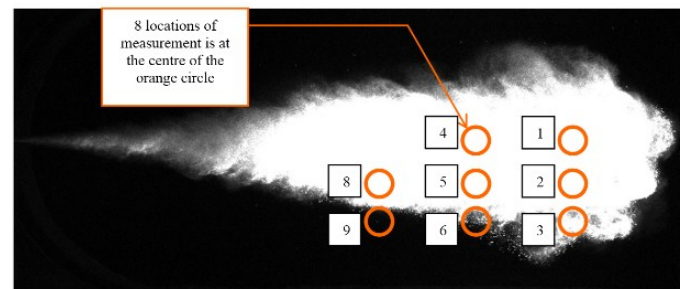


Figure 2. Dropsizes measurements at location 81.3, 101.3 and 121.3 mm axially and 0, 8 and 16 mm offset.

Simulation set up

The internal volume of the HPSC was replicated in Star-CD v.3.26 CFD software (see Figure 3). All meshes were hexahedral and the volume was manually built using a custom script. The minimum mesh length is 0.333 mm which corresponds to a

volume of 0.037 mm^3 . The total number of mesh cells is 3,728,480 which is limited by the amount of computer memory available.

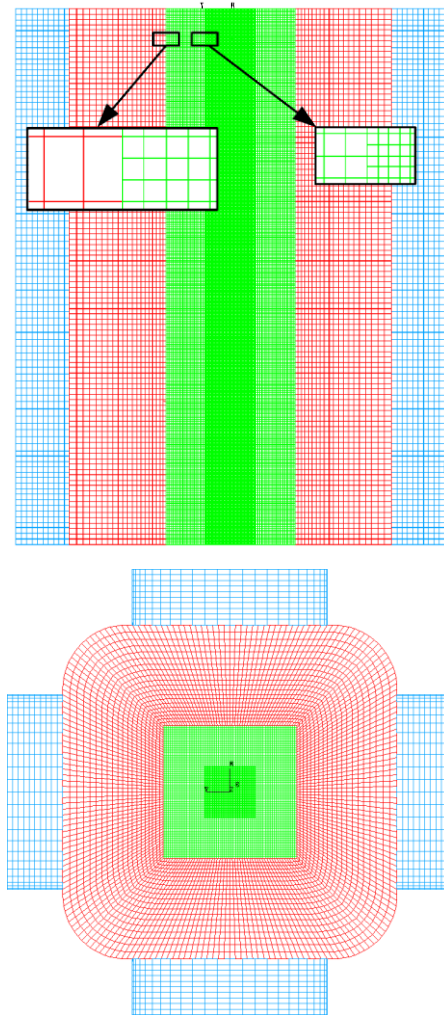


Figure 3. Cross-section and top down view of the HPSC mesh detailing the varying mesh resolution. Minimum cell size is 0.333 mm .

The evaluation of various spray models that led to the final configuration shown in Table 1 is detailed in [10].

Category	Model	Configuration
Droplet injection	Blob atomisation	8.5° half cone angle, initial drop size $240 \mu\text{m}$
Secondary breakup	KH-RT breakup	$C_3=1, B_0=0.61, B_1=6$
Collision model	Mesh Independent O'Rourke (MIOC)	Nordin's constraint; Aamir and Watkins timescale correction; and neighbour cell search level = 2;
Droplet drag	Dynamic TAB	$C_b = 0.5, C_{D1} = 5.0, C_f = 1/3, C_k = 8.0$
Turbulence model	LES	$k-l$ SGS model, $C_k=0.05, C_\epsilon=1.0$
Particle/Gas phase interaction	Coupling method	Vertex
Injection		Average 109 MPa with custom pressure profile taken from experiment data
Gas pressure		$20, 30, 40 \text{ bar}$ at 25°C

Table 1. Star-CD v3.26 simulation specification.

The simulation boundary conditions are the inner walls of the HPSC and the nozzle exit where droplets are injected using the Blob atomisation model [6]. The detailed in-nozzle physics were not modelled directly. Instead, the injection pressure profile was taken from experimental data and the initial spray diameter was assumed to be the same as the nozzle diameter. Magnified experimental images taken at the nozzle exit region did not show any spray contraction. A timestep of $1 \mu\text{s}$ is used throughout.

A Kelvin-Helmholtz/Rayleigh Taylor (KH/RT) breakup model [11-13] was implemented into StarCD v3.26 in FORTRAN language using the droplet breakup subroutine 'drobrk.f' [6]. The original KH/RT model produces a separate child droplet parcel when more than 2% of the parent droplet volume is reduced by stripping. However, this feature was not implemented in Star-CD because the software does not permit the separation of one parcel into multiple parcels, so the parcel droplet size was reduced uniformly.

The LES and $k-\epsilon$ RANS turbulence models were compared [10]. LES produced distinct 'wavy' patterns and droplet clustering similar to images captured in experiment. With RANS, spray formation is a symmetrical plume.

The location and frequency of inter-droplet collisions were analysed. As expected, collision is most likely to occur in the dense droplet regions (see Figure 4).

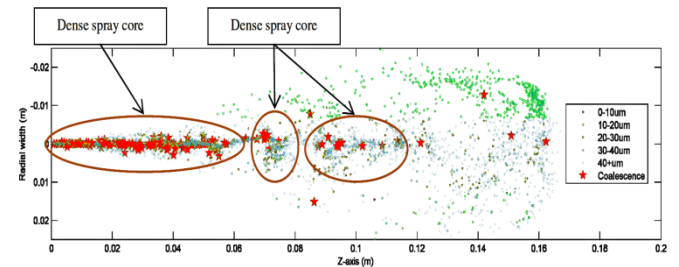


Figure 4. Collision locations highlighted in red stars of a simulated spray, $p = 30 \text{ bar}$; $t = 8 \text{ ms}$.

Mesh Independent O'Rourke Collision Model

It has been shown [10,14,15] that in the O'Rourke collision model [16] prediction of droplet collision rate is dependent on cell size. This significantly affects the mean droplet size and Sauter Mean Diameter (SMD). In order to overcome this problem, a custom method of calculating the control volume for collision was formulated. In Lagrangian-Eulerian simulation, the discrete phase (droplet phase) is represented in the form of parcels. Each parcel contains numerous droplets with the same physical properties. In a numerical simulation of the collision between two droplets, two parcels impact rather than two individual droplets. In the Mesh Independent O'Rourke Collision Model (MIOC) the control volume for collision modelling is a sphere which is large enough to occupy the space of the two colliding parcels when they are just about to collide. Further details are given in [10].

Results and discussion

Figure 5 shows an image of the spray taken at 5 ms after start of injection (top) compared with the simulated spray at the same condition. The gas pressure was 40 bar and the spray was lit with the light sheet. A cross-section of the simulated spray (using LES) was selected and the droplet surface area was calculated to represent the brightness intensity in order to replicate the experimental image, which was taken using scattered light from the light sheet. The simulation image (bottom) shows details of the spray disintegrating from a straight jet (at $< 30 \text{ mm}$ from nozzle exit) to a more wavy and chaotic structure.

Comparing the two images, both of them show similar structure with the experimental image appearing to have a higher fidelity compared with the simulation image. The overall shape, penetration and width of the two sprays are similar.

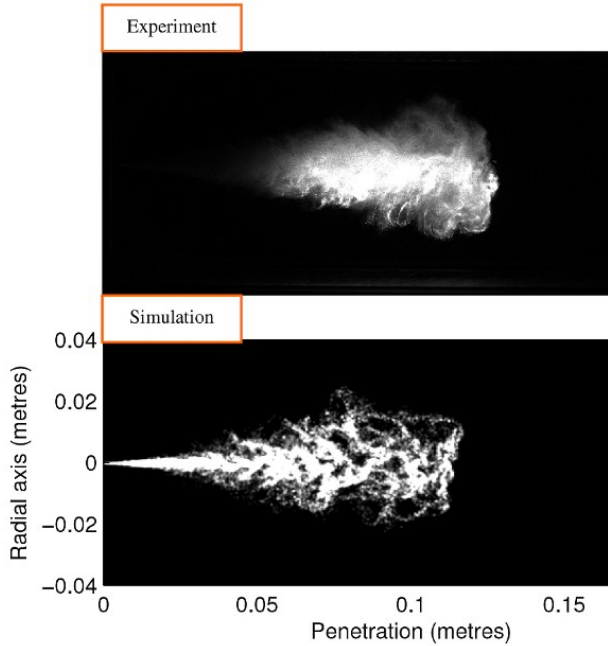


Figure 5. A spray image (top) compared with the equivalent simulation result (bottom), $p=40$ bar, $t=5$ ms

Penetration results

Figure 6 is a log-log plot of the spray penetration with respect to time from the experimental results and simulation results.

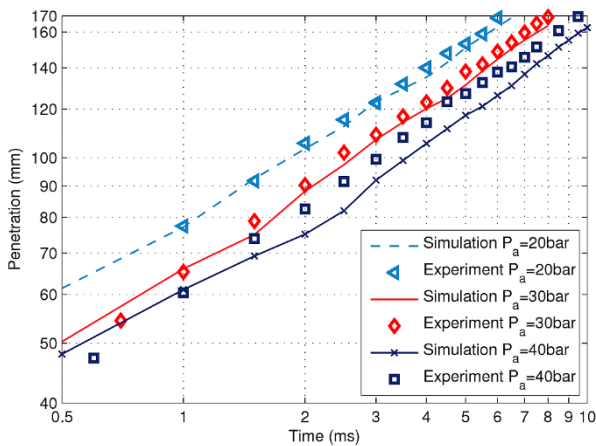


Figure 6. A log-log plot of the spray penetration against time after injection start for both experimental (dots) and simulation (lines) results.

Both experiment and simulation show a very similar penetration rate. The results show the penetration rate is affected by the gas density with higher density resulting in slower penetration.

Cone angle results

Figure 7 shows a plot of the spray average cone angle with respect to time of both simulation and experimental results. As can be seen in Figure 5 the outline of the spray is irregular and so no single overall cone angle is apparent. For each of around 1000 positions along the spray axis of each the pre-processed images the spray half angle was calculated, on each side of the central axis. The overall spray half cone angle was taken as the mean of the individual angles. The two half cone angles were averaged and the average of all the shots taken.

The cone angle is affected by the gas density with higher chamber pressure leading to a wider spray. The experimental results show a cone angle of about 8 to 9° at the beginning expanding to about 10° at 5 ms before reducing to around 9° again from 8 ms onwards. The contraction at very long spray durations is because the spray widening slows while penetration continues to increase thus resulting in a narrower overall average cone angle.

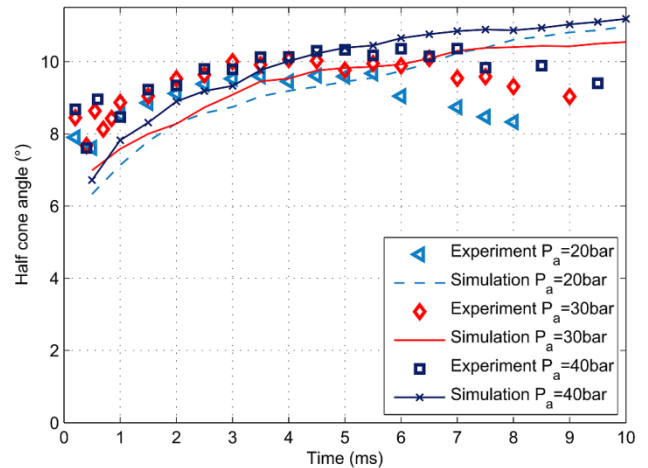


Figure 7. Half cone angle from experiment and simulation

In the simulation results, the difference between the cone angle at 20 and 30 bar is not that obvious. Moreover, at durations greater than 7 ms the 20 bar cone angle is shown to be wider than at 30 bar. The difference between experiment and simulation is more obvious in the cone angle results. The simulation results show a much narrower early spray than the experiments. Even though the initial spray cone angle for the simulations is larger than the experimental values, the simulated spray in the region of the nozzle widens at a slower rate than the real spray, so that overall simulated spray angle is less than experimental angles. However, after a few ms, the simulated spray begins to widen at a faster rate than the real spray. From 6 ms after start of injection, the simulated cone angle continues to increase while the experimental cone angle begins to contract. The differences in spray angle in the early spray are probably due to limitations on minimum cell size. The nozzle exit region requires a finer resolution to capture the details of the high shear rates between the jet flow and surrounding gas. Attempts to reduce mesh size below 0.333mm results in simulation instability. This is because the Eulerian/Lagrangian multi-phase simulation code requires the volume occupied by the droplets to be much less than the cell volume. In the near nozzle region where the droplet density is high, reducing cell size below 0.333mm results in the volume fraction of the discrete phase in some cells being much too high.

Dropsizes results

The experimental results from the eight locations show no significant influence of the sampling location on the Sauter Mean Diameter (SMD). The droplet imaging method only allows dropsizes measurements in relatively sparse regions, where drop breakup and collision are no longer significant. Further, no significant influence of chamber pressure on SMD was found. Details of the measurement of dropsizes are given in [9].

Table 2 shows a summary of the arithmetic mean dropsizes and the SMD of the simulation and experimental results. The experimental results showed that the SMD ranged from 22.4 to 23.6 μm . The RMS of the results ranged from 8.2 to 9.0 μm and the droplet count ranged from 1075 to 2407. The simulation results showed very similar SMD ranging from 23.6 to 24.3 μm and RMS ranging from 7.7 to 9.2 μm . The arithmetic mean

shows a significant difference of around 4.5 μm between simulation and experiment results. This might be caused by the limitation in Star-CD software in grouping droplets into a parcel [10].

Air pressure	20 bar		30 bar		40 bar	
Result type	Sim	Exp	Sim	Exp	Sim	Exp
Mean (μm)	18.7	14.2	18.3	13.8	17.8	13.3
SMD (μm)	23.6	22.4	23.9	23.6	24.3	22.7
RMS	7.7	8.2	8.3	9.0	9.2	8.6
Sample size	13434	1612	10951	2407	11855	1075

Table 2. Mean droplet size and SMD results of the simulation compared with experimental data.

Figure 8 shows a cross-sectional view of SMD and a fuel volume isosurface plot of a spray at 10 ms after start of injection with 20 bar chamber pressure. It can be seen that beyond about 40 mm from the nozzle the SMD essentially remains unchanged and there is no persistent core of high droplet diameter. Shot to shot variations in the distribution of the droplet clusters would lead to approximately the same value of SMD being measured at any location in the dilute spray, which correlates with the experimental findings.

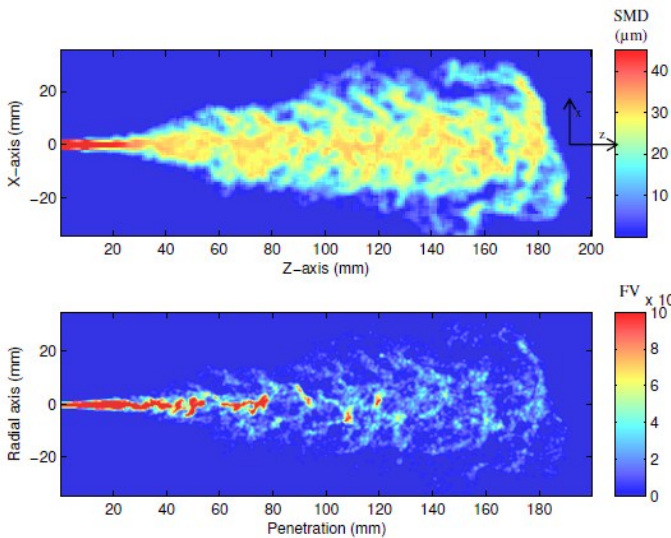


Figure 8. SMD cross-section and fuel volume surface plot at 10 ms after start of injection, 20 bar chamber pressure.

Conclusions

The simulation results showed that the modelled penetration, cone angle and mean drop sizes of the respective sprays were predominantly accurate when compared with experimental results. However, the spray cone angle comparison showed a significantly narrower spray in the early stages of injection compared with the simulations. It is speculated that the cell volume lower limit (inherent in the Lagrangian/Eulerian modelling method) and hardware memory limit contributed to the cone angle discrepancy. A full Eulerian simulation of the early spray would reduce the lower limit on cell size which would in turn allow smaller scale motions to be solved explicitly in the LES approach.

Most of the spray breakup and droplet collisions (potentially leading to coalescence) occur relatively close to the nozzle, so in the more dilute regions of the spray the droplet size will show poor correlation with sampling position.

References

- [1] Baumgarten, C., Mixture Formation in Internal Combustion Engines. Series: Heat and Mass Transfer 2006: Springer.
- [2] Faeth, G., L. Hsiang and P. Wu, Structure and Breakup Properties of Sprays, *Int. J. Multiphase Flow*, 1995, **21**: pp 99-127.
- [3] Gorokhovski, M. and M. Herrmann, Modeling Primary Atomisation, *Annual Reviews in Fluid Mechanics*, 2008, **40**: pp 343-366.
- [4] Villermaux, E., Fragmentation, *Annual Review of Fluid Mechanics*, 2007, **39**: pp 419-446.
- [5] Pope, S.B., Turbulent Flows 2000: Cambridge University Press.
- [6] CD_Adapco_Group, Methodology, StarCD Version 3.26, 2006.
- [7] Lesieur, M., O. Metais and P. Comte, Large-Eddy Simulations of Turbulence 2005: Cambridge University Press.
- [8] Kosaka, H. and S. Kimura, LES of Diesel Fuel Spray, in *ICLASS*, 2006.
- [9] Goldsworthy, L., C. Bong and P. Brandner, Measurements of Diesel Spray Dynamics and the Influence of Fuel Viscosity, using PIV and Shadowgraphy, *Atomisation and Sprays*, 2011, **21**(2): pp 167-178.
- [10] Bong, C., Numerical and Experimental Analysis of Diesel Spray Dynamics including the Effects of Fuel Viscosity, 2010. PhD thesis, University of Tasmania
- [11] Taylor, G.I., The Instability of Liquid Surfaces when Accelerated in a Direction Perpendicular to their Planes, *The Scientific Papers of Sir Geoffery Ingram Taylor*, 1963, **3**: pp 532-536.
- [12] Su, T.F., M.A. Patterson, R.D. Reitz, and P.V. Farrell, Experimental and Numerical Studies of High Pressure Multiple Injection Sprays, *SAE. 960861*, 1996.
- [13] Ricart, L.M., J. Xin, G.R. Bower, and R.D. Reitz, In-Cylinder Measurement and Modeling of Liquid Fuel Spray Penetration in a Heavy-Duty Diesel Engine. SAE. 971591, *SAE 971591*, 1997.
- [14] Schmidt, D.P. and C.J. Rutland, Reducing Grid Dependency in Droplet Collision Modeling. *Journal of Engineering for Gas Turbines and Power*, 2004, **126**: pp 227-233.
- [15] Munnannur, A., Droplet Collision Modeling in Multi-Dimensional Engine Spray Computations, in Department of Mechanical Engineering. 2007, University of Wisconsin - Madison: Madison., in Department of Mechanical Engineering, University of Wisconsin, Madison, 2007
- [16] O'Rourke, P.J., Collective Drop Effects on Vaporising Liquid Sprays, in Princeton University, 1981